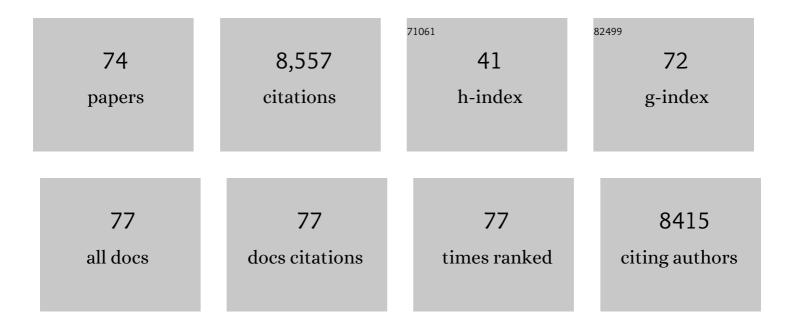
## Xue Wang

## List of Publications by Year in descending order

Source: https://exaly.com/author-pdf/5409924/publications.pdf Version: 2024-02-01



XUE WANC

#	Article	IF	CITATIONS
1	CO <sub>2</sub> electrolysis to multicarbon products at activities greater than 1 A cm <sup>â^'2</sup> . Science, 2020, 367, 661-666.	6.0	860
2	Platinum-based nanocages with subnanometer-thick walls and well-defined, controllable facets. Science, 2015, 349, 412-416.	6.0	854
3	Molecular tuning of CO2-to-ethylene conversion. Nature, 2020, 577, 509-513.	13.7	682
4	CO <sub>2</sub> electrolysis to multicarbon products in strong acid. Science, 2021, 372, 1074-1078.	6.0	541
5	Palladium–platinum core-shell icosahedra with substantially enhanced activity and durability towards oxygen reduction. Nature Communications, 2015, 6, 7594.	5.8	440
6	Cooperative CO2-to-ethanol conversion via enriched intermediates at molecule–metal catalyst interfaces. Nature Catalysis, 2020, 3, 75-82.	16.1	390
7	Efficient electrically powered CO2-to-ethanol via suppression of deoxygenation. Nature Energy, 2020, 5, 478-486.	19.8	363
8	Pd@Pt Core–Shell Concave Decahedra: A Class of Catalysts for the Oxygen Reduction Reaction with Enhanced Activity and Durability. Journal of the American Chemical Society, 2015, 137, 15036-15042.	6.6	296
9	Pt-Based Icosahedral Nanocages: Using a Combination of {111} Facets, Twin Defects, and Ultrathin Walls to Greatly Enhance Their Activity toward Oxygen Reduction. Nano Letters, 2016, 16, 1467-1471.	4.5	228
10	High-Energy-Surface Engineered Metal Oxide Micro- and Nanocrystallites and Their Applications. Accounts of Chemical Research, 2014, 47, 308-318.	7.6	203
11	Hydroxide promotes carbon dioxide electroreduction to ethanol on copper via tuning of adsorbed hydrogen. Nature Communications, 2019, 10, 5814.	5.8	201
12	High carbon utilization in CO2 reduction to multi-carbon products in acidic media. Nature Catalysis, 2022, 5, 564-570.	16.1	197
13	Efficient electrocatalytic conversion of carbon monoxide to propanol using fragmented copper. Nature Catalysis, 2019, 2, 251-258.	16.1	188
14	3D metal-organic framework as highly efficient biosensing platform for ultrasensitive and rapid detection of bisphenol A. Biosensors and Bioelectronics, 2015, 65, 295-301.	5.3	181
15	Efficient Methane Electrosynthesis Enabled by Tuning Local CO <sub>2</sub> Availability. Journal of the American Chemical Society, 2020, 142, 3525-3531.	6.6	154
16	Efficient upgrading of CO to C3 fuel using asymmetric C-C coupling active sites. Nature Communications, 2019, 10, 5186.	5.8	127
17	Enhancing the Photocatalytic Activity of Anatase TiO <sub>2</sub> by Improving the Specific Facetâ€Induced Spontaneous Separation of Photogenerated Electrons and Holes. Chemistry - an Asian Journal, 2013, 8, 282-289.	1.7	115
18	High-Rate and Efficient Ethylene Electrosynthesis Using a Catalyst/Promoter/Transport Layer. ACS Energy Letters, 2020, 5, 2811-2818.	8.8	106

XUE WANG

#	Article	IF	CITATIONS
19	Controlled Synthesis and Enhanced Catalytic and Gasâ€Sensing Properties of Tin Dioxide Nanoparticles with Exposed Highâ€Energy Facets. Chemistry - A European Journal, 2012, 18, 2283-2289.	1.7	103
20	High-efficiently visible light-responsive photocatalysts: Ag3PO4 tetrahedral microcrystals with exposed {111} facets of high surface energy. Journal of Materials Chemistry A, 2013, 1, 12635.	5.2	100
21	CO <sub>2</sub> Electroreduction to Formate at a Partial Current Density of 930 mA cm <sup>–2</sup> with InP Colloidal Quantum Dot Derived Catalysts. ACS Energy Letters, 2021, 6, 79-84.	8.8	100
22	Controlled synthesis of concave Cu <sub>2</sub> O microcrystals enclosed by {hhl} high-index facets and enhanced catalytic activity. Journal of Materials Chemistry A, 2013, 1, 282-287.	5.2	98
23	Low coordination number copper catalysts for electrochemical CO2 methanation in a membrane electrode assembly. Nature Communications, 2021, 12, 2932.	5.8	97
24	Efficient electrosynthesis of n-propanol from carbon monoxide using a Ag–Ru–Cu catalyst. Nature Energy, 2022, 7, 170-176.	19.8	96
25	Carbon-efficient carbon dioxide electrolysers. Nature Sustainability, 2022, 5, 563-573.	11.5	95
26	Promoting CO2 methanation via ligand-stabilized metal oxide clusters as hydrogen-donating motifs. Nature Communications, 2020, 11, 6190.	5.8	93
27	Silica-copper catalyst interfaces enable carbon-carbon coupling towards ethylene electrosynthesis. Nature Communications, 2021, 12, 2808.	5.8	91
28	Synthesis and shape-dependent catalytic properties of CeO2 nanocubes and truncated octahedra. CrystEngComm, 2012, 14, 7579.	1.3	88
29	Hollow Metal Nanocrystals with Ultrathin, Porous Walls and Wellâ€Controlled Surface Structures. Advanced Materials, 2018, 30, e1801956.	11.1	83
30	A metal-supported single-atom catalytic site enables carbon dioxide hydrogenation. Nature Communications, 2022, 13, 819.	5.8	83
31	Mesoporous Mn3O4–CoO core–shell spheres wrapped by carbon nanotubes: a high performance catalyst for the oxygen reduction reaction and CO oxidation. Journal of Materials Chemistry A, 2014, 2, 3794.	5.2	81
32	Carbonate ions-assisted syntheses of anatase TiO2 nanoparticles exposed with high energy (001) facets. RSC Advances, 2012, 2, 3251.	1.7	80
33	Response Characteristics of Bisphenols on a Metal–Organic Framework-Based Tyrosinase Nanosensor. ACS Applied Materials & Interfaces, 2016, 8, 16533-16539.	4.0	72
34	Gold-in-copper at low *CO coverage enables efficient electromethanation of CO2. Nature Communications, 2021, 12, 3387.	5.8	70
35	Rational design and synthesis of noble-metal nanoframes for catalytic and photonic applications. National Science Review, 2016, 3, 520-533.	4.6	63
36	The synergy between atomically dispersed Pd and cerium oxide for enhanced catalytic properties. Nanoscale, 2017, 9, 6643-6648.	2.8	63

XUE WANG

#	Article	IF	CITATIONS
37	Formaldehyde-assisted synthesis of ultrathin Rh nanosheets for applications in CO oxidation. CrystEngComm, 2013, 15, 6127-6130.	1.3	55
38	Understanding the Thermal Stability of Palladium–Platinum Core–Shell Nanocrystals by <i>In Situ</i> Transmission Electron Microscopy and Density Functional Theory. ACS Nano, 2017, 11, 4571-4581.	7.3	53
39	Electrochemical biosensing platform based on amino acid ionic liquid functionalized graphene for ultrasensitive biosensing applications. Biosensors and Bioelectronics, 2014, 62, 134-139.	5.3	51
40	Ternary Alloys Enable Efficient Production of Methoxylated Chemicals via Selective Electrocatalytic Hydrogenation of Lignin Monomers. Journal of the American Chemical Society, 2021, 143, 17226-17235.	6.6	43
41	Synthesis of layered protonated titanate hierarchical microspheres with extremely large surface area for selective adsorption of organic dyes. CrystEngComm, 2012, 14, 7715.	1.3	42
42	Direct in Situ Observation and Analysis of the Formation of Palladium Nanocrystals with High-Index Facets. Nano Letters, 2018, 18, 7004-7013.	4.5	42
43	Functional Nanochannels for Sensing Tyrosine Phosphorylation. Journal of the American Chemical Society, 2020, 142, 16324-16333.	6.6	42
44	CO <sub>2</sub> Electroreduction to Methane at Production Rates Exceeding 100 mA/cm <sup>2</sup> . ACS Sustainable Chemistry and Engineering, 2020, 8, 14668-14673.	3.2	41
45	Highly Strong and Solvent-Resistant Cellulose Nanocrystal Photonic Films for Optical Coatings. ACS Applied Materials & Interfaces, 2021, 13, 17118-17128.	4.0	41
46	Control of Anatase TiO <sub>2</sub> Nanocrystals with a Series of Highâ€Energy Crystal Facets via a Fuorineâ€Free Strategy. Chemistry - an Asian Journal, 2012, 7, 2538-2542.	1.7	39
47	Electroosmotic flow steers neutral products and enables concentrated ethanol electroproduction from CO2. Joule, 2021, 5, 2742-2753.	11.7	37
48	Synthesis of spatially uniform metal alloys nanocrystals via a diffusion controlled growth strategy: The case of Au-Pd alloy trisoctahedral nanocrystals with tunable composition. Nano Research, 2012, 5, 618-629.	5.8	36
49	What Is Hidden Behind Schiff Base Hydrolysis? Dynamic Covalent Chemistry for the Precise Capture of Sialylated Glycans. Journal of the American Chemical Society, 2020, 142, 7627-7637.	6.6	33
50	Truncated concave octahedral Cu <sub>2</sub> O nanocrystals with { <i>hkk</i> } high-index facets for enhanced activity and stability in heterogeneous catalytic azide–alkyne cycloaddition. Green Chemistry, 2018, 20, 832-837.	4.6	31
51	Study on Thermoelectric Properties of Polycrystalline SnSe by Ge Doping. Journal of Electronic Materials, 2017, 46, 3182-3186.	1.0	29
52	Dopant-tuned stabilization of intermediates promotes electrosynthesis of valuable C3 products. Nature Communications, 2019, 10, 4807.	5.8	26
53	Ga doping disrupts C-C coupling and promotes methane electroproduction on CuAl catalysts. Chem Catalysis, 2022, 2, 908-916.	2.9	24
54	Direct Electrochemical Tyrosinase Biosensor based on Mesoporous Carbon and Co <sub>3</sub> O <sub>4</sub> Nanorods for the Rapid Detection of Phenolic Pollutants. ChemElectroChem, 2014, 1, 808-816.	1.7	21

XUE WANG

#	Article	IF	CITATIONS
55	Visible and Reversible Restrict of Molecular Configuration by Copper Ion and Pyrophosphate. ACS Sensors, 2020, 5, 2438-2447.	4.0	21
56	Understanding the Stability of Ptâ€Based Nanocages under Thermal Stress Using <i>In Situ</i> Electron Microscopy. ChemNanoMat, 2018, 4, 112-117.	1.5	19
57	Scalable Synthesis of Palladium Icosahedra in Plug Reactors for the Production of Oxygen Reduction Reaction Catalysts. ChemCatChem, 2016, 8, 1658-1664.	1.8	18
58	Atomistic insights into the nucleation and growth of platinum on palladium nanocrystals. Nature Communications, 2021, 12, 3215.	5.8	18
59	Shape-controlled synthesis of CO-free Pd nanocrystals with the use of formic acid as a reducing agent. Chemical Communications, 2016, 52, 12594-12597.	2.2	17
60	Facile Synthesis of Pt–Pd Alloy Nanocages and Pt Nanorings by Templating with Pd Nanoplates. ChemNanoMat, 2016, 2, 1086-1091.	1.5	16
61	Concentrated Ethanol Electrosynthesis from CO <sub>2</sub> via a Porous Hydrophobic Adlayer. ACS Applied Materials & Interfaces, 2022, 14, 4155-4162.	4.0	15
62	Nucleation-mediated synthesis and enhanced catalytic properties of Au–Pd bimetallic tripods and bipyramids with twinned structures and high-energy facets. Nanoscale, 2016, 8, 2819-2825.	2.8	14
63	A surfactant free synthesis and formation mechanism of hollow Cu <sub>2</sub> O nanocubes using Cl <sup>â^'</sup> ions as the morphology regulator. RSC Advances, 2015, 5, 61421-61425.	1.7	11
64	One-Step Synthesis of Supported High-Index Faceted Platinum–Cobalt Nanocatalysts for an Enhanced Oxygen Reduction Reaction. ACS Applied Energy Materials, 2020, 3, 5077-5082.	2.5	11
65	Toward affordable and sustainable use of precious metals in catalysis and nanomedicine. MRS Bulletin, 2018, 43, 860-869.	1.7	9
66	An electrochemical deoxyribonucleic acid biosensor for rapid genotoxicity screening of chemicals. Analytical Methods, 2015, 7, 3347-3352.	1.3	6
67	Highly Efficient Separation of Methylated Peptides Utilizing Selective Complexation between Lysine and 18-Crown-6. Analytical Chemistry, 2020, 92, 15663-15670.	3.2	5
68	Sensing Mechanism of <scp>Excited‣tate</scp> Intermolecular Hydrogen Bond for Phthalimide: Indispensable Role of Dimethyl Sulfoxide. Chinese Journal of Chemistry, 2021, 39, 1113-1120.	2.6	3
69	Self-assembly gel-based dynamic response system for specific recognition of N-acetylneuraminic acid. Journal of Materials Chemistry B, 2021, 9, 4690-4699.	2.9	1
70	Bioinspired Sialic Acid Regulated Ion Nanochannel. Advanced Materials Interfaces, 0, , 2200186.	1.9	1
71	High-efficiency two-dimensional separation of natural products based on β-cyclodextrin stationary phase working in both hydrophilic and reversed hydrophobic modes. Journal of Chromatography A, 2022, 1673, 463069.	1.8	1
72	Aspartic Acid-Modified Phospholipids Regulate Cell Response and Rescue Memory Deficits in APP/PS1 Transgenic Mice. ACS Chemical Neuroscience, 2022, 13, 2154-2163.	1.7	1

#	Article	IF	CITATIONS
73	Scalable Synthesis of Palladium Icosahedra in Plug Reactors for the Production of Oxygen Reduction Reaction Catalysts. ChemCatChem, 2016, 8, 1602-1602.	1.8	Ο
74	Shape-controlled synthesis of metal oxides micro/nanocrystals enclosed by crystal facets of high surface energy. Scientia Sinica Chimica, 2013, 43, 1630-1639.	0.2	0